Electronic Supplementary Material (ESI) for Journal of Materials Chemistry A.

Supporting information

Hollow-ZIFs-Templated Formation of ZnO@C-N-Co Core-Shell Nanostructure for Highly Efficient Pollutant Photodegradation

Huirong Chen, Kui Shen,* Junying Chen, Xiaodong Chen and Yingwei Li*

Key Laboratory of Fuel Cell Technology of Guangdong Province, School of Chemitry and Chemical Engineering , South China University of Technology, Guangzhou 510640, P. R. China

E-mail: cekshen@scut.edu.cn *(K. S.);* liyw@scut.edu.cn *(Y. L.)*

Figure Captions

Figure S1. XRD patterns of the sample obtained by pyrolyzing the hollow Zn/Co-ZIF at 550 °C (denoted as Zn/Co-ZIF-550) and at 700 °C (denoted as Zn/Co-ZIF-700).

Figure S2. (a) Low- and (b) high-resolution TEM images, STEM image (c) and EDS mappings (d-h) of the sample prepared by pyrolyzing the hollow Zn/Co-ZIF at 550 °C.

Figure S3. (a) Low- and (b) high-resolution TEM images of the hollow carbon-cobalt-based structure obtained at 700 °C.

Figure S4. (a) and (b) TEM images of the as-prepared ZnO@C-N-Co.

Figure S5. (a) SEM image, (b) and (c) TEM images of ZIF-67. (d) SEM image, (e) and (f) TEM images of ZIF-67-600.

Figure S6. (a) SEM image, (b) and (c) TEM images of ZIF-8. (d) SEM image, (e) and (f) TEM images of ZIF-8-600.

Figure S7. (a) SEM image, (b) and (c) TEM images of ZnO.

Figure S8. TG curves of the as-sythesized ZIF-67, ZIF-8, and hollow Zn/Co-ZIF.

Figure S9. XPS survey spectrums of ZIF-67, ZIF-8, hollow Zn/Co-ZIF, and commercial pure ZnO.

Figure S10. A magnified TEM image of Figure 5b.

Figure S11. UV-vis absorption spectras of the photocatalytic degradation of MO in the presence of (a) ZnO@C-N-Co, (b) ZnO, (c) ZIF-8-600, and (d) ZIF-67-600, respectively. Inset of (a) shows the molecular structural formula of MO.

Figure S12. UV-vis absorption spectras of the photocatalytic degradation of MO in the absence of catalyst (a) and without light (b).

Figure S13. UV-Vis spectra of the adsorption of MO using the ZIF-8-600, ZnO@C-N-Co, ZIF-67-600, and pure ZnO as adsorbent.

Captions for Tables

Table S1. Physicochemical properties of ZnO@C-N-Co, ZIF-8-600 and ZIF-67-600.

Table S2. Experiment of degradation of MO.

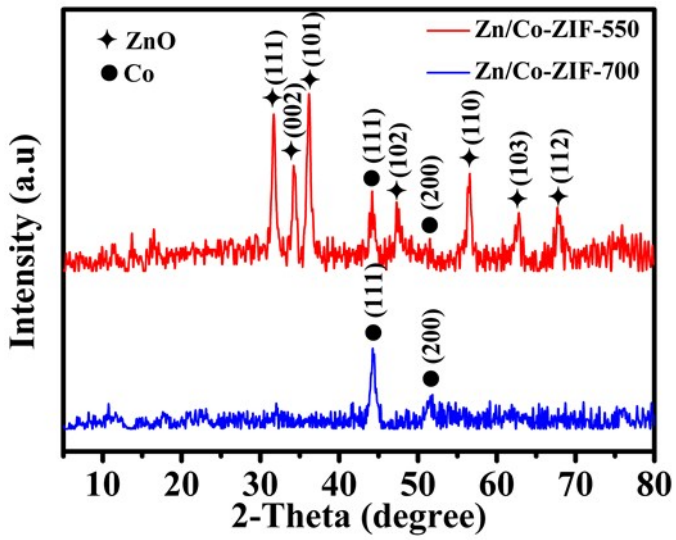

Figure S1. XRD patterns of the samples obtained by pyrolyzing the hollow Zn/Co-ZIF at 550 °C (denoted as Zn/Co-ZIF-550) and at 700 °C (denoted as Zn/Co-ZIF-700).

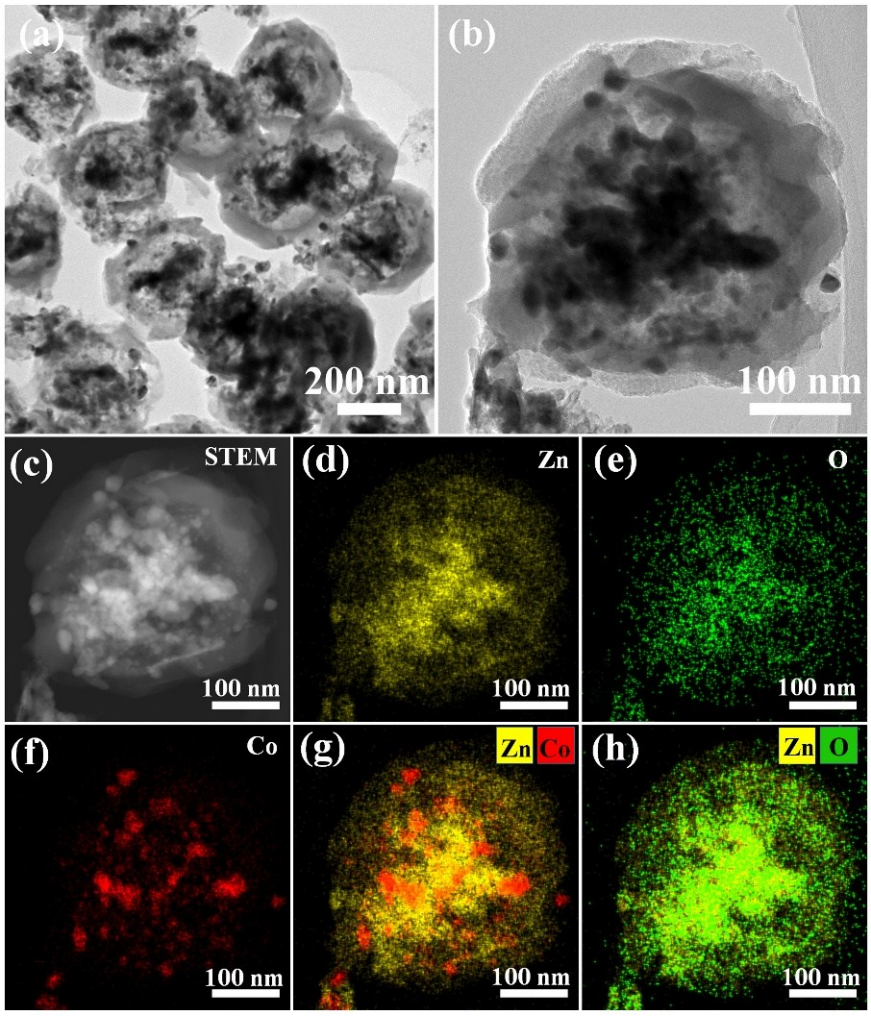

Figure S2. (a) Low- and (b) high-resolution TEM images, STEM image (c) and EDS mappings (d-h) of Zn/Co-ZIF-550.

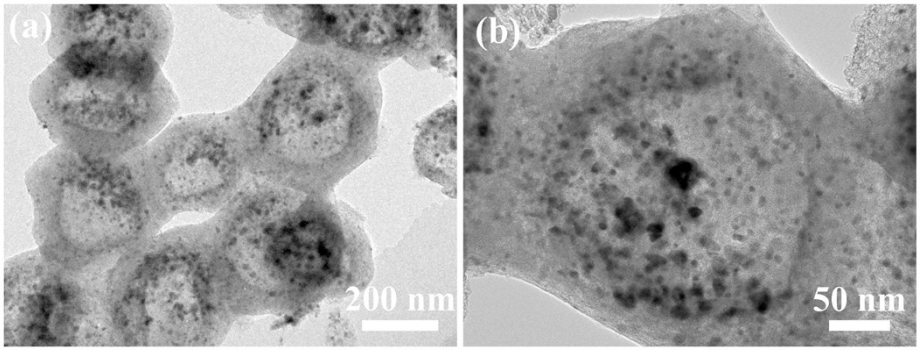

Figure S3. (a) Low- and (b) high-resolution TEM images of Zn/Co-ZIF-700.

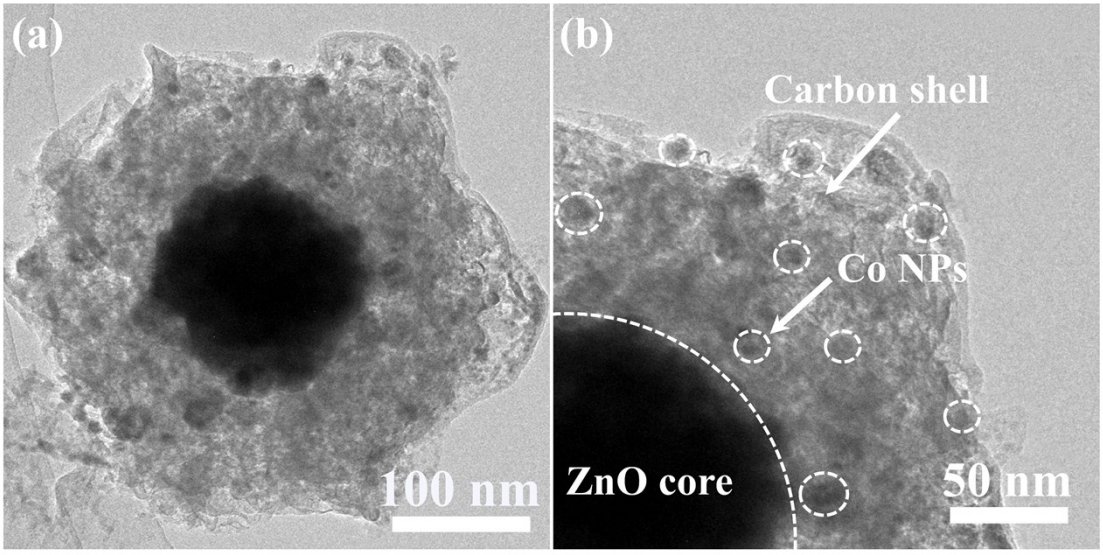

Figure S4. (a) and (b) TEM images of the as-prepared ZnO@C-N-Co.

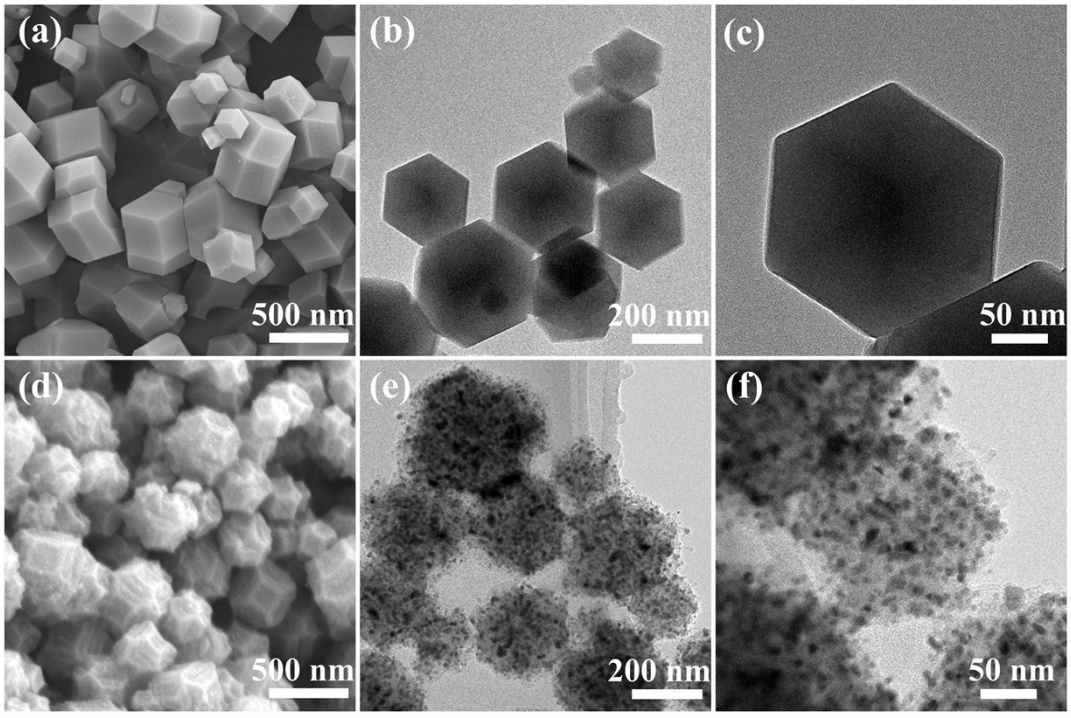

Figure S5. (a) SEM image, (b) and (c) TEM images of ZIF-67. (d) SEM image, (e) and (f) TEM images of ZIF-67-600.

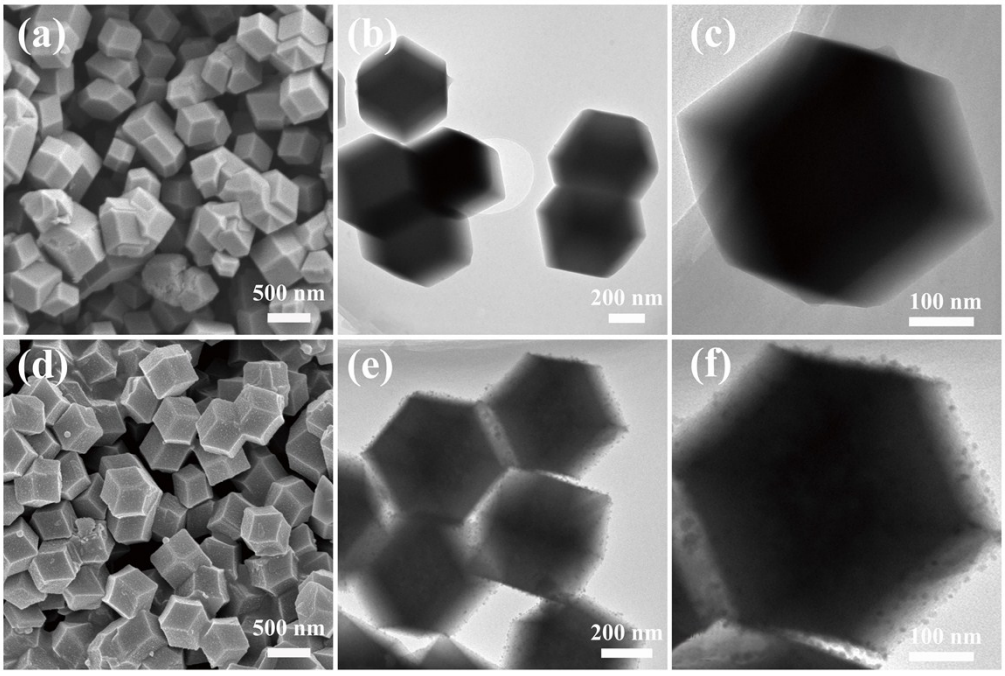

Figure S6. (a) SEM image, (b) and (c) TEM images of ZIF-8. (d) SEM image, (e) and (f) TEM images of ZIF-8-600.

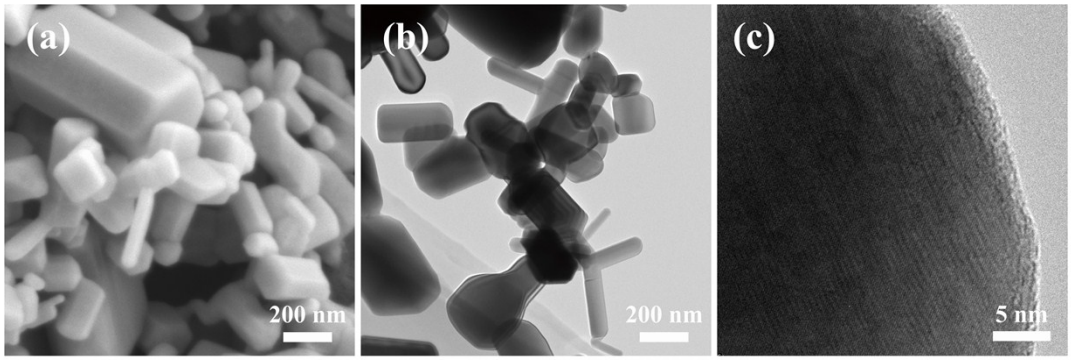

Figure S7. (a) SEM image, (b) and (c) TEM images of ZnO.

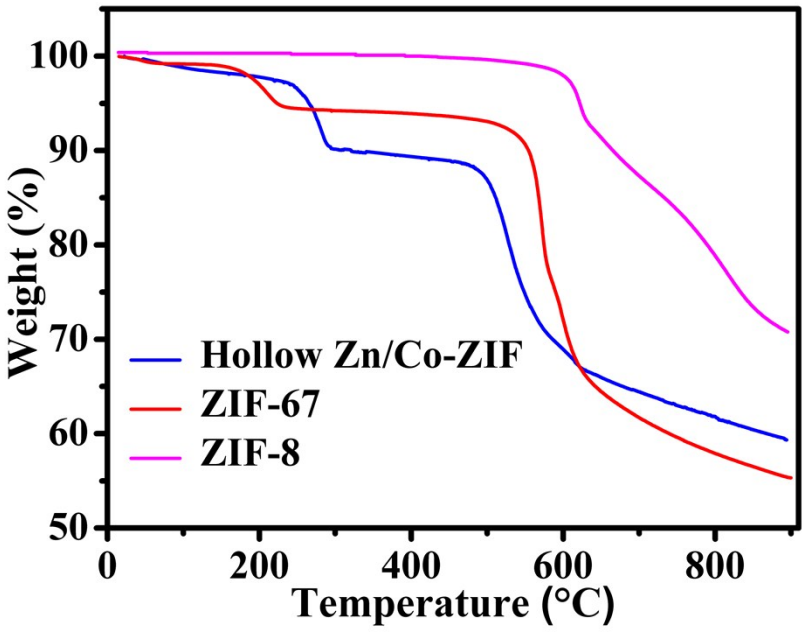

Figure S8. TG curves of the as-sythesized ZIF-67, ZIF-8, and hollow Zn/Co-ZIF.

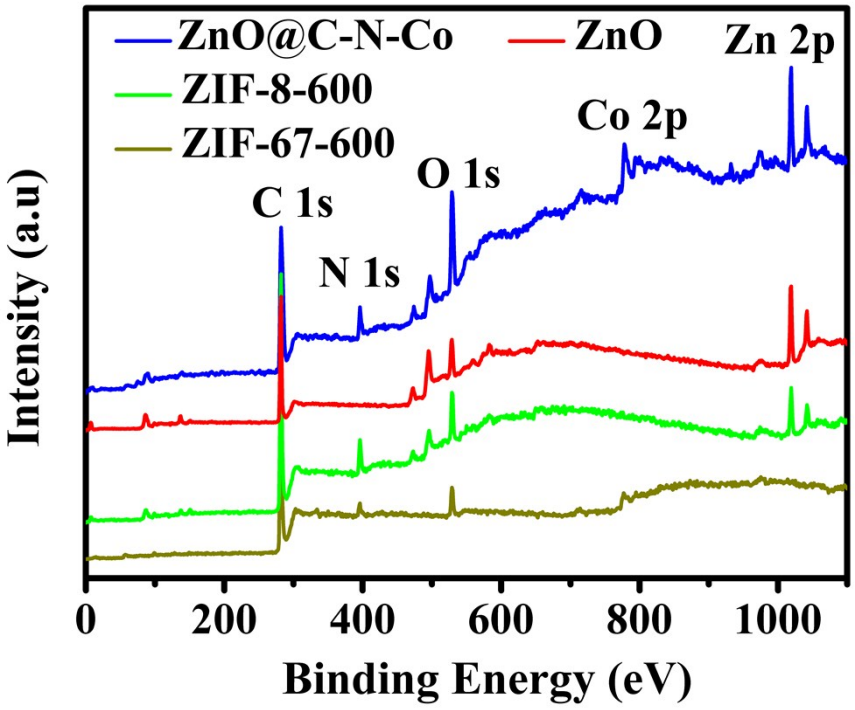

Figure S9. XPS survey spectra of ZIF-67, ZIF-8, hollow Zn/Co-ZIF, and commercial pure ZnO.

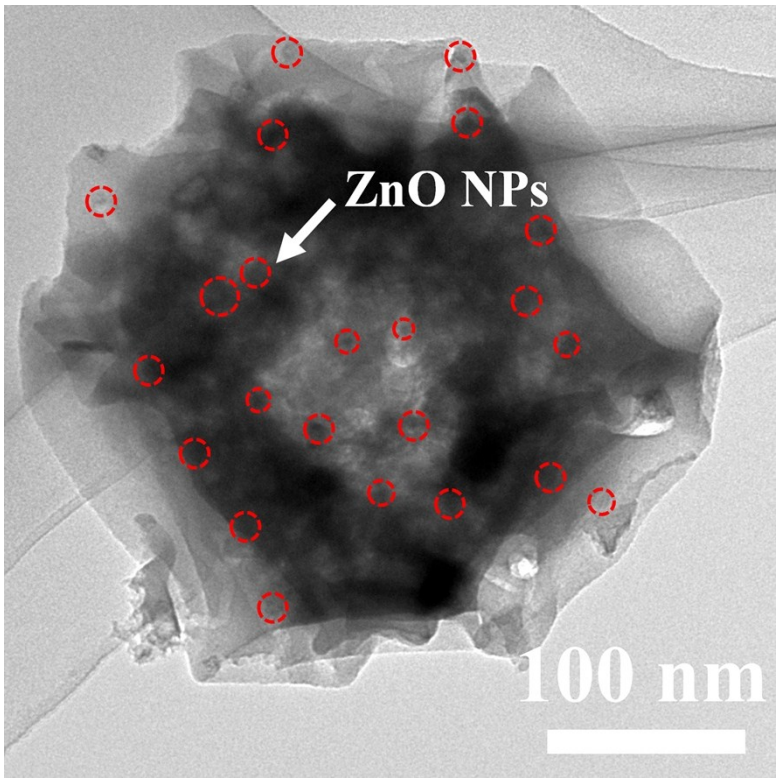

Figure S10. A magnified TEM image of Figure 5b.

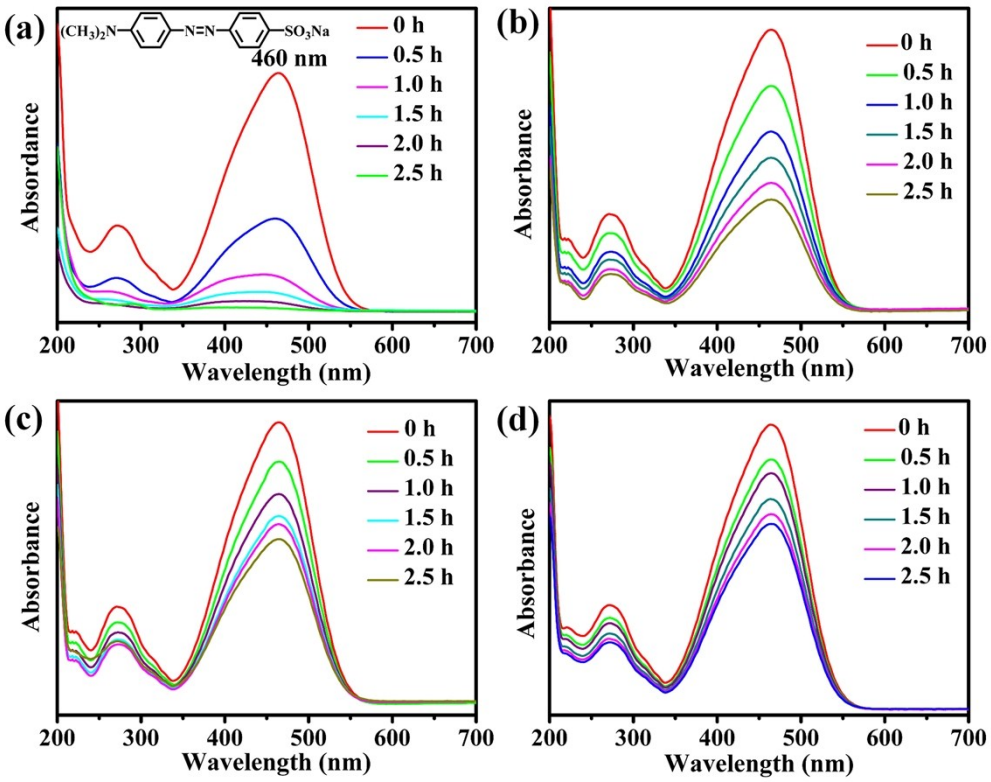

Figure S11. UV-vis absorption spectra of the photocatalytic degradation of MO in the presence of (a) ZnO@C-N-Co, (b) ZnO, (c) ZIF-8-600, and (d) ZIF-67-600, respectively. Inset of (a) shows the molecular structural formula of MO.

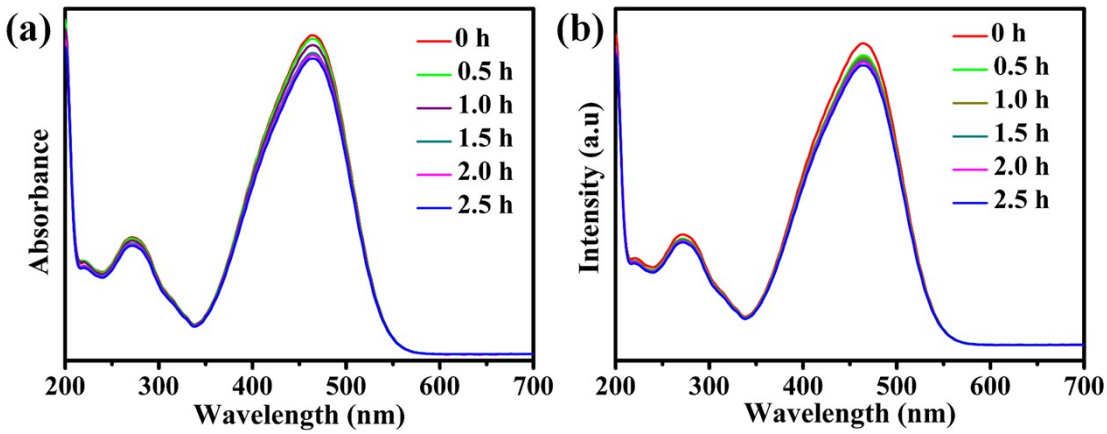

Figure S12. UV-vis absorption spectra of the photocatalytic degradation of MO in the absence of catalyst (a) or without light (b).

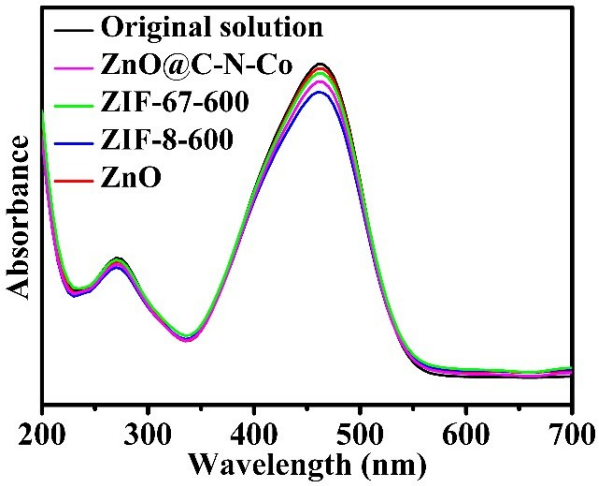

Figure S13. UV-vis spectra of MO aqueous solution before and after adding various samples to compare their adsorption capability.

Table S1. Physicochemical properties of ZnO@C-N-Co, ZIF-8-600 and ZIF-67-600.

Catalyst	Co loading[a] (wt %)	Zn loading[a] (wt %)	S_{BET}[b] (m^2g^{-1})	Pore volume[c] (m^3g^{-1})	Mesopore volume[d] (m^3g^{-1})	Mesopore size[e] (nm)
ZnO@C-N-Co	10.9	25.7	188	0.36	0.34	10.5
ZIF-8-600	/	29.4	728	0.43	0.04	13.8
ZIF-67-600	37.8	/	316	0.23	/	/

[a)]Measured by AAS. [b)]S_{BET} is calculated by the Brunauer-Emmett-Teller equation. [c)] Total pore volume is determined by using the adsorption branch of the N_2 isotherm at P/P_0=0.99. [d)] Msopore volume is obtained from the BJH cumulative specific absorption volume of pore 1.70-300.00 nm diameter. [e)]Mesopore diameter is determined from the local maximum of the BJH distribution of pore diameters obtained in the adsorption branch of the N_2 isotherms.

Table S1. Experiment of degradation of MO.

Items	C/C_0[a]					
	t=0 h	t=0.5 h	t=1.0 h	t=1.5 h	t=2.0 h	t=2.5 h
ZIF-67-600	1.000	0.885	0.821	0.781	0.734	0.706
ZIF-8-600	1.000	0.822	0.720	0.658	0.606	0.581
ZnO	1.000	0.715	0.607	0.505	0.442	0.398
ZnO@C-N-Co	1.000	0.369	0.148	0.070	0.025	0.005
Under light without catalyst	1.000	0.996	0.984	0.974	0.960	0.958
No ligtht with ZnO@C-N-Co catalyst	1.000	0.961	0.952	0.945	0.937	0.928

[a)]C and C_0 are the initial concentration after the equilibrium adsorption and the reaction concentration of methyl orange, respectively.